ELSEVIER

Journal of Organometallic Chemistry 549 (1997) 177–186

Journal of Organometallic Chemistry

Metallocene dichlorides bearing acenaphthyl substituted cyclopentadienyl rings: preparation and polymerization behavior

Timo Repo [a,*], Gerhard Jany [a], Kimmo Hakala [b], Martti Klinga [a], Mika Polamo [a], Markku Leskelä [a], Bernhard Rieger [c]

[a] *Department of Chemistry, Laboratory of Inorganic Chemistry, P.O. Box 55, University of Helsinki, Helsinki FIN-00014, Finland*
[b] *Polymer Science Centre, Helsinki University of Technology, P.O. Box 356, Espoo FIN-02151, Finland*
[c] *Abteilung Anorganische Chemie II, Molekülchemie und Katalyse, Universität Ulm, Ulm D-89069, Germany*

Received 6 June 1997; received in revised form 10 July 1997

Abstract

The unbridged complex [bis(η^5-7,9-diphenylcyclopenta[*a*]acenaphthadienyl)] zirconium dichloride (**8**) and two asymmetric ethylene bridged metallocenes {bis[1,2-(η^5-7,9-diphenylcyclopenta[*a*]acenaphthadienyl)-1-phenyl] ethane} zirconium dichloride (**9**) and {[1-(η^5-7,9-diphenylcyclopenta[*a*]acenaphthadienyl)-2-phenyl-2-(η^5-9-fluorenyl)] ethane} zirconium dichloride (**10**) were prepared and used as catalysts for ethene and propene homopolymerization after activation with MAO. Whereas zirconocenes **8** and **9**, that bear two acenaphthyl substituted Cp-rings, have only moderate activity, **10** produces polyethene with high activity and high molecular weight. In propene polymerization only atactic polymer was formed and the chain termination occurred mainly via β-methyl elimination. The solid state structures of compounds **8**, **9** and **10** were determined by means of X-ray diffraction analysis. © 1997 Elsevier Science S.A.

Keywords: Zirconium; Metallocene; Catalysis; Polymerization; Ethene; Propene

1. Introduction

Since the discovery of methylaluminumoxane (MAO) as cocatalyst in the middle of 1970s [1–3], Group 4 metallocenes turned out to be very effective catalyst precursors for homogeneous α-olefin polymerization and attracted therefore considerable attention. Metallocenes offer a useful method to control the polymer properties, since modifications in the ligand framework have a direct influence on the polymerization behavior of the catalytic active metal center. [1] With these catalyst systems, depending on the substitution pattern of the Cp-rings and thus symmetry of metal complexes, polymers with different kind of microstructures and compositions can be produced. In propene polymerization e.g., the level of stereocontrol can be adjusted from atactic to highly isotactic or syndiotactic polypropenes via innumerable intermediate microstructures [4–6].

Part of our interest has been concentrated on the preparation and polymerization behavior of metallocenes carrying large substituents, like tetraphenylcyclopentadienyl or 7,9-diphenylcyclopenta[*a*]acenaphthadienyl (ACp) moieties [7–9]. In this paper we present the preparation and crystal structure of three new bridged and unbridged zirconocene dichlorides, all carrying the sterically demanding ACp moiety. The influence of its large α- and β-substituents on the polymerization behavior is demonstrated by homopolymerization reactions of ethene and propene with the MAO activated metallocenes.

2. Results and discussion

2.1. Ligand preparation

In previous papers it was shown that epoxides can be converted to a variety of ligand precursors and this synthetic approach is especially useful for the preparation of ethylene bridged complexes bearing two different cyclopentadienyl fragments [7–14]. This route was successfully utilized in the preparation of the ligand

* Corresponding author. E-mail: timo.repo@helsinki.fi.

[1] The role of metallocene catalysts in polymerization has been lately reviewed (see Refs. [4–6]).

PII S0022-328X(97)00524-X

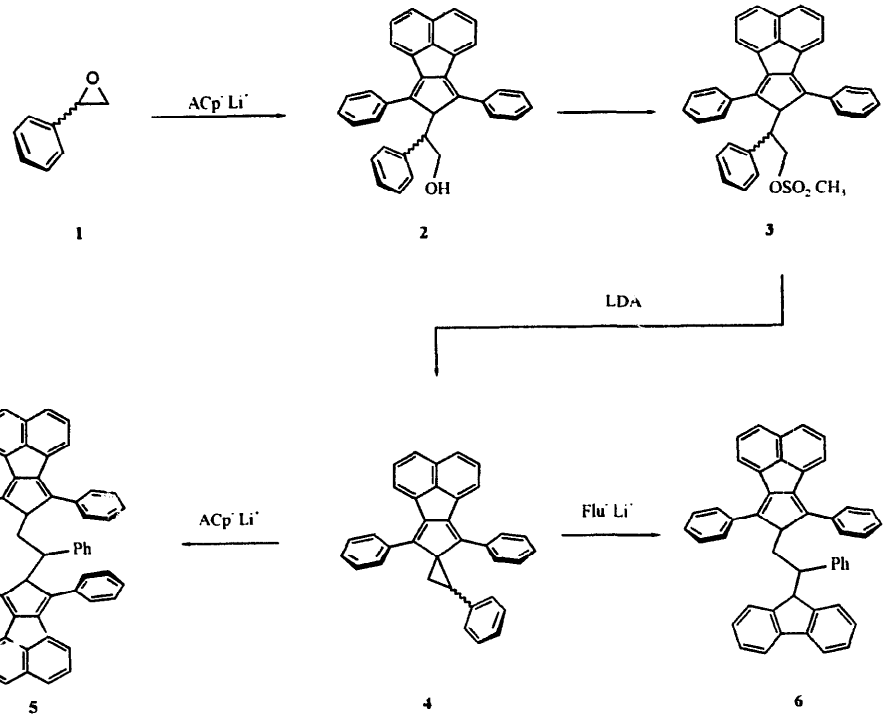

Scheme 1. Ring opening of **4** with ACp or fluorenyl anions results in the ligand precursors **5** and **6**.

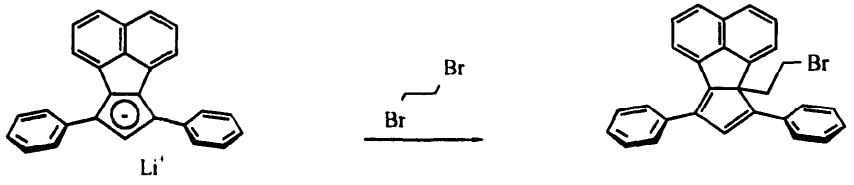

Scheme 2. Reaction of ACp⁻ Li⁺ with dibromo ethane yields to monosubstitution at 3-position.

precursors **5** and **6**, starting from a nucleophilic ring opening of epoxystyrene (**1**) with ACp anion. The formed primary alcohol (**2**) was further transferred into the corresponding methanesulfonate derivative (**3**), from which the formation of spiro[(2-phenylcyclopropane)-1,1′-(7,9-diphenylcyclopenta[*a*]acenaphthadiene)] (**4**) was accomplished with lithium diisopropyl amide (Scheme 1). By this synthetic approach the intermediate compound **4** can be prepared in reasonable yields as described by us earlier [8].

The nucleophilic ring opening of **4** with ACp or fluorenyl anions occurs regiospecific and leads to the ligand precursors **5** and **6**, respectively. In compound **6** the phenyl substituent of the bridge is located in α-position to the incoming fluorenyl unit, corresponding to results reported before [7–14]. In order to prepare a ligand precursor similar to **6**, containing the phenyl group in vicinal position to the ACp unit, a ring opening reaction of spiro-(1-phenylcyclopropane-9,9′-fluorene) (**7**) [11] should be carried out with ACp lithium, following the similar route as described above. The reaction of **7** with ACp lithium was unsuccessful and gave after work-up only the unreacted starting materials, maybe due to the low nucleophility of the ACp anion. Also attempts to synthesize a ligand precursor similar to **5**, but without a phenyl substituent in the ethylene backbone, were not successful. Treatment of 1,2-dibromo ethane with 2 equiv. of ACp lithium led only to mono substitution of one bromide with ACp at the sterically and electronically unfavored 3-position of the ACp unit (Scheme 2) [15]. [2]

2.2. *Complex formation and solid state structures*

The preparation of the unbridged complex [bis(η^5-7,9-diphenylcyclopenta[*a*]acenaphthadienyl)] zirconium dichloride (**8**) was performed by the reaction of ACp^-Li^+ with $ZrCl_4$ at −78°C in CH_2Cl_2 and the complex was isolated in good yields. Treatment of $ZrCl_4$ with dilithio salts of ligand precursors **5** and **6** in dichloro

[2] Similar substitution at 3-position was also observed when ring opening of **4** was performed with strong nucleophiles (see Ref. [16]).

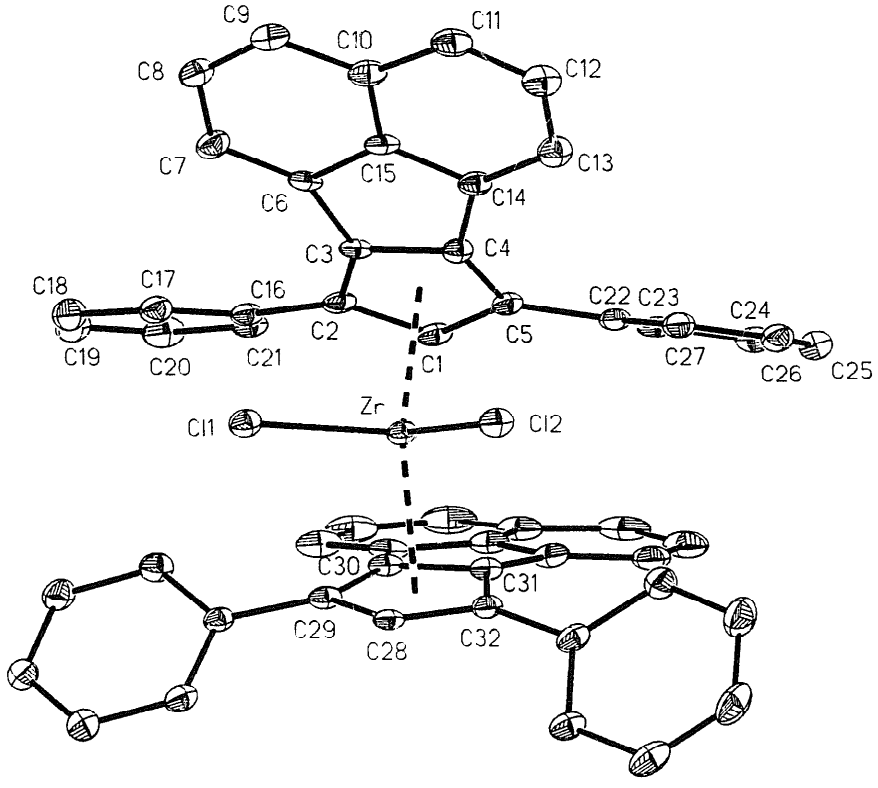

Fig. 1. Molecular structure of **8** with displacement ellipsoids drawn at 30% probability level. The solvent molecules and hydrogen atoms were omitted for clarity reasons.

methane gave after work-up the asymmetric ethylene bridged metallocenes, {bis[1,2-(η^5-7,9-diphenylcyclopenta[*a*]acenaphthadienyl)-1-phenyl] ethane} zirconium dichloride (**9**) and {[1-(η^5-7,9-diphenylcyclopenta[*a*]acenaphthadienyl)-2-phenyl-2-(η^5-9-fluorenyl)] ethane} zirconium dichloride (**10**) with moderate isolated yields. Crystals suitable for X-ray analysis of **8–10** were obtained from saturated chloroform solution and the molecular structures of **8**, **9** and **10** are displayed in Figs. 1–4. Based on the structures of **9** and **10** the phenyl substituent of the bridge is occupying the energetically favored equatorial orientation of the metallacycles verifying earlier observations [7,10].

In the solid state the acenaphthyl groups of complex **8** are pointing into opposite directions with equal distances between the ACp centroids and Zr-atom. This staggered orientation allows an almost ideal η^5-coordination to one of the Cp-rings (C(28)–C(32)), while the coordination of the other (C(1)–C(5)) is slightly distorted. [3] The unsubstituted carbon atom C(1) is 0.146 Å closer to the metal center than the acenaphthyl substi-

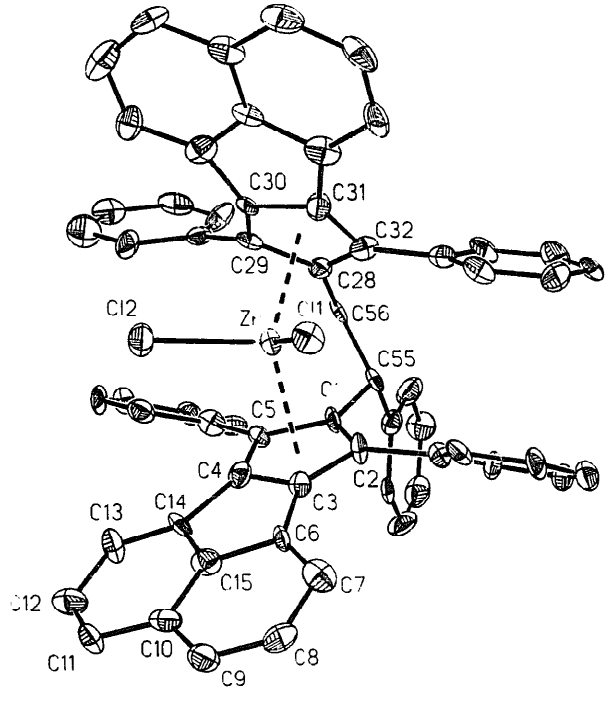

Fig. 2. Molecular structure of **9** with displacement ellipsoids drawn at 30% probability level. The solvent molecules and hydrogen atoms were omitted for clarity reasons.

[3] A similar unequal coordination mode was observed for unbridged Flu_2ZrCl_2 but in higher extent. In this complex one fluorenyl moiety can be regarded as η^5-coordinated while the other, having a more severe distribution in coordination than the ACp-moiety of **8**, can be regarded as η^3-coordinated to the metal center (see Ref. [17]).

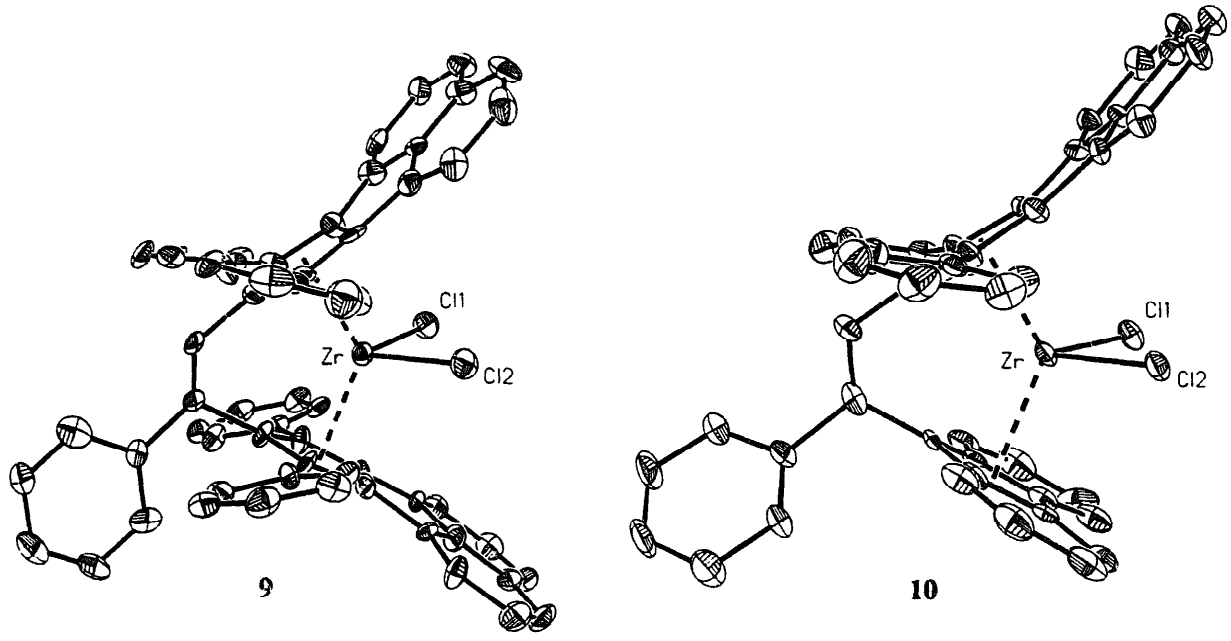

Fig. 3. The side views of complex **9** and **10** reveal the opening of the ligand frameworks and that the phenyl rings in α-position do not significantly interfere with the coordination sites of the metal centers.

tuted carbons of the Cp-ring C(3) and C(4), indicating unequal coordination of Cp-carbons to the metal ion (Table 1).

In complex **9** the ethylene bridge forces both ACp units to orientate so that the acenaphthyl substituents are pointing into the same, frontal direction and the phenyl

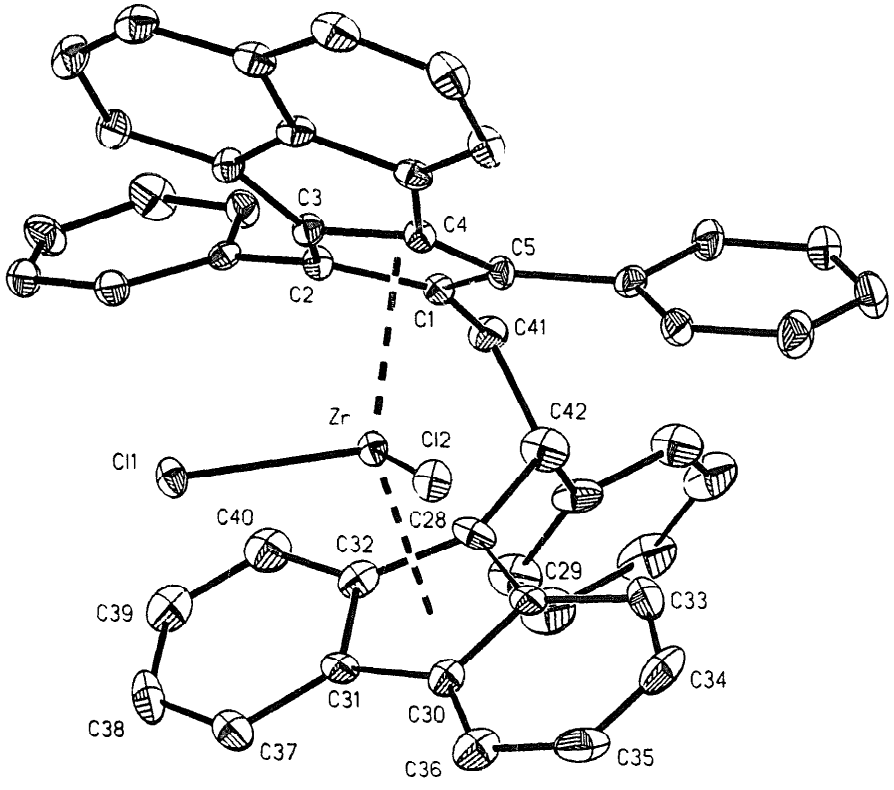

Fig. 4. Molecular structure of **10** with displacement ellipsoids drawn at 30% probability level. The hydrogen atoms were omitted for clarity reasons.

Table 1
Distances between zirconium and carbon atoms of the Cp-rings [Å]

	8	9	10
Zr-(1)	2.470(7)	2.535(12)	2.509(8)
Zr-(2)	2.535(6)	2.559(13)	2.573(9)
Zr-(3)	2.616(6)	2.597(12)	2.586(9)
Zr-(4)	2.616(7)	2.559(13)	2.559(9)
Zr-(5)	2.555(7)	2.512(13)	2.525(8)
Zr-(28)	2.510(6)	2.525(13)	2.439(8)
Zr-(29)	2.562(6)	2.578(12)	2.590(8)
Zr-(30)	2.564(6)	2.547(12)	2.692(9)
Zr-(31)	2.563(7)	2.590(13)	2.683(8)
Zr-(32)	2.584(6)	2.550(14)	2.515(9)

substituents of the Cp-rings are settled down above each other, but no distortion in the pseudotetrahedral geometry around the zirconium center was observed. The distances of the ACp centers to zirconium are almost equal, corresponding to the values found for **8** (Table 2). In comparison to the unbridged complex **8**, the ethylene bridge in **9** forces the Centr–Zr–Centr angle to be opened about 6.4°.

The λ-angle, which describes the inclination of the line through the Zr and Cp-center from the Cp-plane, can be regarded as an indication about the extent of hapticity (η) in the zirconium ligand bonding [19]. In complex **10** the ACp unit has an almost ideal η^5-coordination to the metal center, but the λ-angle of the fluorenyl centroid is reflecting a decreased hapticity instead (Table 2). In case of zirconocenes, the distance between metal center and the carbon atoms of the Cp-system, if it exceeds 2.8 Å, has been discussed as a non-bonding interaction. [3] In **10** two carbon atoms of one fluorenyl moiety (C(28)–C(32)) have an elongated carbon–Zr bonding (C(30) 2.692(9) Å and C(31) 2.683(8) Å) indicating a distortion in the coordination mode, but the Cp ring can still be considered as η^5-coordinated (Table 1). However, the bonding distances between the Zr–ACp and the Zr–fluorenyl centroid differ only slightly from each other.

The opening of the ligand framework is described by the θ angle which is the angle between the two Cp-planes. Even though the Centr–Zr–Centr angle of com-

Table 2
Bonding parameters of zirconocenes **8**, **9**, and **10** compared to Cp_2ZrCl_2

	8	9	10	Cp_2ZrCl_2 [d]	
Centr1–Zr	2.256	2.248	2.245	2.198	[Å]
Centr2–Zr	2.253	2.251	2.280	2.202	[Å]
Centr1–Zr–Centr2	119.4	125.8	127.6	128.3	[°]
λ, Centr1–Zr[a]	85.7	87.7	87.8	88.6	[°]
λ, Centr2–Zr[a]	89.1	88.9	82.8	88.7	[°]
θ[b]	52.1	57.3	61.5	53.5	[°]
Torsion angle[c]	–	50.2(13)	43.6(12)	–	[°]
Zr–Cl(1)	2.430(3)	2.429(4)	2.415(3)	2.4477(12)	[Å]
Zr–Cl(2)	2.410(2)	2.421(4)	2.414(3)	2.4444(13)	[Å]
Cl–Zr–Cl	93.55(9)	91.46(14)	91.90(9)	97.03(5)	[°]

[a] Inclination of the line between the Zr and Cp-centroid from the Cp-ring plane.
[b] Angle between two Cp-planes.
[c] Torsion angles of ethene bridge: For **9** C(1)–C(55)–C(56)–C(28) and for **10** C(1)–C(41)–C(42)–C(28).
[d] Because of two independent molecules in the unit cell, the numbers are given as mean values [18].

Table 3
Ethene polymerization with complexes **8**, **9** and **10**/MAO ([Al]/[Zr] = 2000)

Catalyst	T_p(°C)[a]	n_{cat}(μmol)[b]	p(bar)[c]	Activity[d]	M_W 10^3 g/mol	M_W/M_N	T_{mp}(°C)
8	30	3.0	2.8	440	630	2.82	138.3
	50		3.8	1180	282	2.07	137.7
	70		4.6	1260	181	2.84	135.2
9	30	3.0	2.8	520	128	1.88	136.6
	50		3.8	810	86	1.91	132.9
	70		4.6	1910	41	2.07	132.2
10	30	2.0	2.8	8260	1111	2.84	136.5
	50		3.8	15,400	802	2.75	134.7
	70		4.6	11,800	287	3.02	134.4

[a] Polymerization temperature.
[b] Molar amount of metallocene.
[c] Monomer pressure.
[d] Activity in kg PE(mol[Zr] × h)$^{-1}$.

plex **10** is about two degree larger than for **9** (Table 2), the observed θ angles of the ethylene bridged complexes indicate that **10** exposes a more opened gap around the *cis*-positioned chlorides if compared to **9**.

2.3. Ethene polymerization

All complexes were tested for ethene polymerization at different temperatures and constant monomer concentration (0.34 mol/l) [4] using MAO as cocatalyst. The unbridged complex **8** polymerizes ethene with moderate activity. [5] The productivity of ethylene bridged complex **9** resembles the values obtained for **8**, whereas **10** differs from both of them by higher activity and by ability to produce high molecular weight polyethenes (Table 3). All complexes turned out to be activated only slowly by MAO, e.g., for complex **9** it took about 45 min at 30°C before the polymerization solution turned from yellow to deep violet and ethene consumption started. After activation occurred the ethene consumption was found to be constant, even slightly increasing towards the end of each polymerization run. Above 70°C decomposition of the catalyst systems was observed.

2.4. Propene polymerization

The described complexes were also tested in propene polymerization at different temperatures and constant monomer concentration (0.71 mol/l). [4] At this low monomer concentration complexes **8** and **9** were able to produce only traces of polymer at 50°C, while **10** turned out to be moderately active already at 30°C.

When polymerization temperature was kept constant (50°C) and propene pressure was varied, the activity of the unbridged metallocene **8** increased slowly with the rising monomer concentration, but still its polymerization activity was very low. Under similar conditions the ethylene bridged complexes **9** proved to be considerably more active than **8**, whereas **10** in which one ACp moiety of **9** was replaced by a fluorenyl unit, showed a considerably higher activity (3850 kg PP (mol [Zr] × h)$^{-1}$) than **8** or **9**.

Table 4
Propene polymerization with complexes **8**, **9** and **10**/MAO ([Al]/[Zr] = 2000)[a]

Catalyst	T_p(°C)[b]	p(bar)[c]	Activity[d]	M_w g/mol	M_w/M_n
8	50	4.6	35	5900	1.43
	50	5.7	53	6900	1.50
9	50	4.6	300	9300	1.78
	50	5.7	400	11,100	1.82
10	30	1.4	400	12,800	1.85
	50	2.0	750	4000	1.68
	50	4.6	2480	8500	1.83
	50	5.7	3850	10,300	1.87

[a] Molar amount of catalyst precursors was kept constant 6 μmol.
[b] Polymerization temperature.
[c] Monomer pressure.
[d] Activity in kg PP(mol[Zr]×h)$^{-1}$.

All the MAO activated catalysts, regardless temperature and pressure used, produce low molecular weight atactic polypropenes (Table 4). The short polypropene chains made it possible to use ^{1}H NMR for end group determination. According to ^{1}H NMR spectra, about 90% of chain termination occurred via β-methyl elimination, which has also been confirmed to be the main chain termination mechanism for many other metallocenes having sterically crowded metal center. [6]

2.5. Correlation between complex structure and the polymerization behavior

The highest catalytic activity in the series was observed for complex **10**. Even though the complex is bearing one ACp unit, the productivity of this catalyst precursor is comparable to activities reported for $EtPh(Flu)_2ZrCl_2$ under similar conditions [24]. This observation is in accordance with earlier results revealing that the activity of $EtPh[(ACp)(Cp)]ZrCl_2$ is alike to $EtPh[(Flu)(Cp)]ZrCl_2$ [8,9]. These correlations state that one ACp moiety in the ligand framework does not significantly change the activity if compared to fluorenyl analogues.

Replacement of the fluorenyl group of **10** by a second ACp unit lowers drastically the activities, both, in ethene and propene polymerization. Based on X-ray measurements, the decrease in activity can be visualized as an increased steric repulsion around the zirconium

[4] Ethene and propene concentrations were measured by the use of calibrated mass flow meters. For an appropriate equation of state for the propene/toluene system, see Refs. [20,21]. For ethene/toluene, see Ref. [22].

[5] [bis(η^5-7,9-diphenylcyclopenta[*a*]acenaphthadienyl)] hafnium dichloride was prepared similar to the zirconium analogue. ^{1}H NMR ($CDCl_3$): δ 6.28 (s, 2H), 7.19–8.14 (m, 32H) FAB-MS: In the FAB-MS spectrum of the complex, parent ions of composition $C_{54}H_{34}HfCl_2^+$ were observed in the appropriate isotope ratios at m/e = 929–936 (M^+). The base peak, however, corresponds $C_{27}H_{17}HfCl_2^+$ at m/e = 588–594. HRMS (FAB) calculated for $C_{54}H_{34}HfCl_2$ (^{180}Hf, ^{35}Cl) 932.1500 found 932.1553. The hafnocene complex shows decreased activity by a factor of 6 in ethene polymerization compared to activity of **8**/MAO under the same polymerization conditions.

[6] In ^{1}H NMR, the polymer end group protons give a doublet at 5.05 and a singlet at 4.95 ppm indicating vinyl end groups. Corresponding signals for the vinylidene end groups formed via β-H elimination were also observed (two singlets at 4.65 and 4.73 ppm). The ratio of vinyl to vinylidene signals was found to be 10:1 only slightly depending on the complexes used. For a detailed description of β-methyl elimination, see Ref. [23].

center (Fig. 3). Besides the fact that in the catalyst precursor **9** both coordination sites are shielded by two sterically demanding ACp units, also the θ angle is reduced 4.2° compared to the θ value of **10**. The ligand framework of complex **9** strongly reduces the chiral coordination cage and thus influences the chain growth.

In the unbridged complex **8** the θ angle is slightly reduced (5.2°) and thus its ligand framework should be a little bit more congested than in **9**. Both ethene and propene activities of **8** are lower than values obtained for **9**. Because in **8** the unbridged ACp-rings are able to move in respect of each other, we assume that the freely rotating phenyl rings in the α-positions of the ACp moiety interfere with the plane of Zr and the reactive *cis*-positioned ligand sites. Corresponding disturbance of freely rotating phenyl rings, but in large extent, was observed for metallocenes bearing a tetraphenylcyclopentadienyl moiety [7,9].

An ACp moiety in the ligand framework induces in metallocenes sterical interactions which are effecting on the polymerization properties of such catalyst precursors. We assume that the lack of stereospecificity of the complexes arises from the frontal orientation of the sterically demanding acenaphtyl group, which is disturbing the enantiomorphic site control of the catalysts at the insertion step of the monomer. Steric influences of two substituents at β-position to the bridge head atom increase the non-bonded interactions between the Cp-ring and the growing polymer chain, and raise the energy required for β-H transfer [19]. The geometry of the ligand framework in complexes **8**, **9** and **10** as well as in other complexes mainly containing fluorenyl moieties, e.g., $Me_2Si(Flu)_2ZrCl_2$, favor β-methyl elimination [19], which was, in fact, the major termination mechanism observed for **8**, **9** and **10** in polymerization of propene.

In general, the replacement of hydrogen atoms located in α-position to the bridge head atom by methyl groups tends to reduce the coordination gap around the metal center and hence lowers the extent of 1,2-misinsertions during the polymerization process [25]. [7] In complexes bearing an ACp unit the coordination gap is further decreased with two phenyl substituents in α-position. Based on ^{13}C NMR spectra all polypropene samples produced by metallocenes **8**, **9** and **10** are highly regioregular and no detectable amounts of tail to tail or head to head misinserted propene units were observed.

The molecular weights of all polymers as well as the catalysts activity are increased with rising monomer concentration indicating a shift in the insertion/termination rate. This can be considered as a proof that in complexes **8**, **9** and **10** the chain termination via β-methyl elimination proceeds by mononuclear mechanism as previously discussed by Resconi et al. [19] for metallocenes bearing fluorenyl moieties.

[7] See also Refs. [4–6].

3. Experimental section

3.1. General

Reactions and manipulations with organometallic compounds were carried out under inert argon atmosphere using standard syringe or Schlenk techniques. Solvents were dried and purified under argon prior to use.

The preparation of 7,9-diphenylcyclopenta[*a*]acenaphthadiene (ACp) was carried out by modifying literature procedures [26,27]: Instead of using dry diethyl ether for the reduction of the intermediate 7,9-diphenyl-8-oxo-cyclopenta[*a*]acenaphthen with $LiAlH_4$ (20% yield), wet diethyl ether was used which increased the yield up to 80%. The syntheses of **2**, **3** and **4** were carried out as described earlier [8]. Because of the similar polarity of the ACp to the formed ligands **5** and **6**, the separation of the products from the raw material was difficult and carried out by careful column chromatography.

The ^1H and ^{13}C NMR spectra were measured on a Varian Gemini 2000 MHz NMR spectrometer using TMS as an internal standard. The mass spectra were recorded on a JEOL SX 102. Elemental analyses were carried out in the microanalytical laboratory of the Institute für Anorganische Chemie, Universität Tübingen (Carlo Erba, Model 1106).

3.2. Polymerization procedure

Methylaluminoxane (MAO, 10 wt.% solution in toluene, M = 800 g/mol, Al = 5.3 wt.%) was purchased from Witco. Ethene (grade 3.5 from AGA) and propene (grade 2.8 from AGA) were purified by passing them through columns filled with molecular sieves, CuO and Al_2O_3. Polymerizations were carried out in toluene in a 0.5 dm^3 stainless steel reactor equipped with a propeller-like stirrer. The stirring speed was 400 rpm. Temperature was 30–90°C and partial pressure of monomer 1.4–5.7 bar.

Toluene (300 cm^3) and the cocatalyst were introduced to the nitrogen-purged reactor. The reactor temperature was controlled by circulating water in the reactor jacket. At the polymerization temperature the monomer feed was started. After the equilibrium was reached, polymerization was initiated by pumping a toluene solution of the catalyst (20 ml) into the reactor. During polymerization the partial pressure of monomer

was maintained constant with an electronic pressure controller.

The polymer was separated from solution with methanol containing a small amount of aqueous hydrochloric acid. The product was washed with methanol and dried under vacuum.

3.3. Polymer characterization

A Waters 150-C ALC/GPC operating at 140°C and equipped with three Polymer Laboratories PLgel 10 μm columns was used to determinate the molecular weights (M_W)and molecular weight distributions (M_W/M_N) of the polymers. Solvent 1,2,4-trichloro benzene was applied at a flow rate 1.0 cm^3/min. The columns were calibrated with narrow molecular weight distribution polystyrenes and then with polypropene or linear low density polyethene standards. The melting temperatures of polyethenes were recorded with a Mettler Toledo DSC821 differential scanning calorimeter. The melting endotherms were measured upon re-heating the polymer sample to 160°C with a heating rate of 10°C/min.

3.4. Synthesis of bis[1-2-(7,9-diphenylcyclopenta[a]-acenaphthadienyl)-1-phenyl] ethane (5)

ACp (4.99 g, 14.6 mmol) was dissolved into 100 ml of diethyl ether. The solution was cooled down to 0°C and *n*-butyl lithium (9.1 ml, 14.6 mmol) was added dropwise. The reaction mixture was stirred 1 h in an ice-bath and after this the diethyl ether was removed. The dry yellow lithium salt was dissolved in 100 ml of DMF and the violet/dark red mixture was cooled down to −10°C. The spiro compound **4** (5.4 g, 12.2 mmol) was added and the reaction mixture was then stirred for 48 h. DMF was removed and solid residue extracted with 200 ml of toluene. Collected organic phases were dried over Na_2SO_4. The product was purified by column chromatography using toluene as an eluent. For further purification the ligand was recrystallized from toluene giving **5** as yellow crystals (3.1 g, 3.9 mmol, 32%). mp. 257°C. ^{1}H NMR ($CDCl_3$): δ 1.89–2.15 (m, 2H, $CH_{2,\,bridge}$), 3.10–3.25 (m, 1H, CH_{bridge}), 4.37–4.42 (m, 1H), 4.50 (d, J = 3.34 Hz, 1H, CH_{ACp}), 6.83–7.92 (m, 37H, aromat. H). FDMS: 786 (M^+). Anal. Calcd for $C_{62}H_{42}$: C, 94.62; H, 5.38. Found: C, 94.84; H, 5.28.

3.5. Synthesis of [1-(7,9-diphenylcyclopenta[a]acenaphthadienyl)-2-(9-fluorenyl)-2-phenyl] ethane (6)

Fluorene (1.35 g, 8.1 mmol) was dissolved in tetrahydrofurane (THF) and treated dropwise with *n*-butyl lithium (1.6 M, 5.1 ml, 8.1 mmol) at −78°C. The reaction mixture was stirred 1 h at room temperature. The spiro compound **4** (3.6 g, 8.1 mmol) was dissolved in 50 ml THF and added dropwise to the solution of ACp lithium salt at 0°C. After stirring overnight at ambient temperature the solution was neutralized by the addition of saturated aqueous solution of NH_4Cl. The aqueous phase was extracted with toluene (2 × 100 ml) and the collected organic phases were dried (Na_2SO_4) and the solvent was distilled off. The brownish oily raw material was purified by column chromatography (eluent: toluene/hexane 1:2) and orange-yellow powder was obtained with 58% yield (3.1 g, 5.1 mmol). mp. 118–119°C. ^{1}H NMR ($CDCl_3$): δ 2.29(m, 1H, $CH_{2,\,bridge}$), 2.54 (m, 1H, $CH_{2,\,bridge}$), 3.44(1H, CH_{bridge}), 3.73(d, 1H, CH_{Flu}), 4.84(m, 1H, CH_{ACp}), 6.35–8.02(m, 29H, aromat. H) ppm. EI-MS: 610 (M^+). HRMS(EI) Calcd for $C_{48}H_{34}$: 610.2660. Found: 610.2662.

3.6. Synthesis of [bis(η^5-7,9-diphenylcyclopenta[a]-acenaphthadienyl)]zirconium dichloride (8)

ACp (4.08 g, 11.9 mmol) was dissolved in 70 ml THF and cooled down to −78°C. *n*-Butyl lithium (7.5 ml, 1.6 M, 11.9 mmol) was dropped slowly to the solution and color changed from bright yellow to deep violet. The reaction mixture was allowed to reach room temperature and stirred for 1 h. THF was removed and the dry solid powder cooled down again to −78°C. 40 ml of pre-cooled CH_2Cl_2 (−78°C) (40 ml) was transferred into the reaction flask and $ZrCl_4$ (1.39 g, 6.0 mmol) was added. The reaction mixture was allowed to reach slowly ambient temperature and the stirring was continued over night. The resulting greenish yellow suspension was then filtered through Celite and the volume was reduced to one third. Yellow solid powder was isolated with 18% yield (0.95 g, 1.1 mmol). ^{1}H NMR ($CDCl_3$): δ 6.37(s, 2H, CH_{ACp}), 7.10–7.85 (m, 32H). In the FAB-MS spectrum of **8**, parent ions of composition $C_{54}H_{34}ZrCl_2^+$ were observed in the appropriate isotope ratios at m/e = 841–847 (M^+) and 807–813 (M^+–Cl).

3.7. Synthesis of [bis[1,2-(η^5-7,9-diphenylcyclopenta-[a]acenaphthadienyl)-1-phenyl]ethane] zirconium dichloride (9)

The ligand precursor **5** (1.9 g, 2.4 mmol) was dissolved in 20 ml THF and the solution was cooled down to −78°C and *n*-butyl lithium (3.0 ml, 4.8 mmol) was added dropwise. The color of the solution turned dark red. After 10 min the reaction mixture was allowed to come slowly to ambient temperature and stirring was continued 30 min at room temperature. The solution was cooled down again to −78°C and $ZrCl_4 \cdot (THF)_2$ (0.91 g, 2.4 mmol) was added. The reaction mixture was then slowly the heated up to 60–65°C and stirred at this temperature for 3 h, during which the solution turned to yellow. THF was then removed and toluene

(35 ml) was added and the reaction mixture shortly warmed to 60–65°C. Toluene unsoluble part was filtered off and 20 ml *n*-hexane were added to the red solution. The formed recipitate was filtered-off again . Further addition of *n*-hexane to orange mother liquid gave **9** as yellow crystalline powder (318 mg, 0.34 mmol, 14%). ^{1}H NMR ($CDCl_3$): δ 4.14–4.48 (m, 2H, $CH_{2,\ bridge}$), 5.46–5.56 (m, 1H, CH_{bridge}), 6.62–8.32 (M, 37H). In the FAB-MS spectrum parent ions of composition $C_{62}H_{40}ZrCl_2^+$ were observed in the appropriate isotope ratios at m/e = 945–952 (M^+) and 910–917 (M^+–Cl). Anal. Calcd for $C_{62}H_{40}ZrCl_2$: C, 78.70; H, 4.26; Cl 7.49. Found: C, 78.72; H, 5.44; Cl, 7.31.

3.8. Synthesis of [[1-(η^5-7,9-diphenylcyclopenta[a]-acenaphthadienyl)-2-(η^5-9-fluorenyl)-2-phenyl]ethane] zirconium dichloride (10)

Ligand precursor **6** (2.9 g, 4.8 mmol) was dissolved in diethylether (50 ml) and treated dropwise with *n*-butyl lithium (1.6 M, 5.9 ml, 9.5 mmol) at −78°C. After further stirring 1 h at room temperature the solvent was removed under vacuo and the dilithiosalt was dissolved in pre-cooled dichloro methane (−78°C). $ZrCl_4$ (1.12 g, 4.8 mmol) was added and reaction mixture was allowed slowly to come to room temperature. Reaction mixture was stirred overnight and then heated to 60–65°C for half an hour. Dichloro methane was then removed and the raw product was dissolved in toluene (40 ml). Addition of hexane (2 × 40 ml) precipitated a yellow solid, which was removed by filtration. From the clear solution the red product crystallized out at −20°C in 18% yield (0.66 g, 0.8 mmol). ^{1}H NMR ($CDCl_3$): δ 4.37–4.75 (m, 2H, $CH_{2,\ bridge}$), 5.47–5.64 (m, CH_{bridge}). In the FAB-MS spectrum parent ions of composition $C_{48}H_{32}ZrCl_2^+$ were observed in the appropriate isotope ratios at m/e = 767–774 (M^+). HRMS (FAB) Calcd for $C_{48}H_{32}ZrCl_2$ (^{90}Zr, ^{35}Cl): 768.0936. Found: 768.0905.

3.9. Crystal structure determination

The data sets were collected on a Rigaku AFC7S diffractometer using graphite monochromatized Mo Kα-radiation (0.71073 Å) at 193 K. The intensities were corrected for Lorentz and polarization effects. An experimental absorption correction (psi-scan) for **9** and **10**, and decay correction for **9** (7.4%) and for **10** (5.7%), were carried out. According to standard reflections, only statistical fluctuation less than 2% were observed for **8**. Crystallographic data and other pertinent information are summarized in Table 5.

The structures were solved by direct methods (SHELXTL/PC) and refined by least-squares techniques. Non-hydrogen atoms were refined with anisotropic displacement parameters and hydrogen atoms are on calculated positions (riding model) with fixed displacement parameters (1.3 × that of the host atom). All refinements were performed using SHELXL-93 software [28]. Figures are plotted using SHELXTL/PC program package [29]. In refinement of **8** one $CHCl_3$ solvent molecule labeled as 'C' was fixed with site occupation factor 0.5 due to its location around the center of symmetry. In case of **9** the solvent molecule

Table 5
Crystal data for the complexes **8**–**10**

Complex	**8**	**9**	**10**
Formula	$C_{54}H_{34}Cl_2Zr \times 1.5CHCl_3$	$C_{62}H_{40}Cl_2Zr \times 2CHCl_3$	$C_{48}H_{32}Cl_2Zr$
M_r	1023.48	1185.80	770.86
Crystal color, habit	yellow, prismatic	yellow, prismatic	red, prismatic
Crystal dimension (mm)	0.15 × 0.15 × 0.1	0.25 × 0.15 × 0.05	0.12 × 0.12 × 0.09
Crystal system	triclinic	triclinic	triclinic
Space group	P-1(No. 2)	P-1(No. 2)	P-1(No. 2)
a, Å	12.714(11)	15.482(9)	12.542(7)
b, Å	13.783(12)	12.900(9)	13.354(6)
c, Å	14.133(9)	14.264(11)	12.082(5)
α, deg	115.95(6)	111.05(5)	108.41(4)
β, deg	93.56(7)	98.52(6)	113.93(5)
γ, deg	91.44(8)	95.93(6)	89.12(5)
V, Å^3	2219(3)	2591(3)	1740.4(14)
Z	2	2	2
D_c, g/cm^3	1.532	1.520	1.471
F(000)	1037	1204	788
Reflections collected	6300	6115	8413
Independent reflections	6300	5884	4104
S	1.063	0.998	1.151
*R*1	0.0660	0.0981	0.0788
*wR*2	0.1629	0.1982	0.1723

labeled as 'A/B' has more than one orientation and the site occupation of the major part refined to the value of 0.71(6).

4. Supporting information available

Tables of displacement parameters and complete lists of bond lengths and angles have been deposited at the Cambridge Crystallographic Data Center. A list of observed and calculated structure factors is available from the authors.

Acknowledgements

Financial support from the Academy of Finland is gratefully acknowledged.

References

[1] K.H. Reichert, K.R. Meyer, Macromol. Chem. 169 (1973) 163.
[2] W.P. Long, D.S. Breslow, Liebigs Ann. Chem. (1975) 463.
[3] A. Andersen, H.G. Cordes, J. Herwig, W. Kaminsky, A. Merck, R. Mottweiler, J. Pein, H. Sinn, H.J. Vollmer, Angew. Chem., Int. Ed. Engl. 15 (1976) 630.
[4] H.H. Brintzinger, D. Fischer, R. Mülhaupt, B. Rieger, B. Waymouth, Angew. Chem., Int. Ed. Engl. 34 (1995) 1143.
[5] M.J. Bochmann, Chem. Soc., Dalton Trans. (1996) 225.
[6] W. Kaminsky, Macromol. Chem. Phys. 197 (1996) 3907.
[7] B. Rieger, R. Fawzi, M. Steimann, Chem. Ber. 125 (1992) 2373.
[8] B. Rieger, T. Repo, G. Jany, Polym. Bull. 35 (1995) 87.
[9] B. Rieger, T. Repo, G. Jany, in: H. Werner, J. Sundermeyer (Eds.), Stereoselective Reactions of Metal-Activated Molecules, Vieweg and Sohn Verlag: Braunschweig/Wiesbaden, 1995, p. 161.
[10] B. Rieger, G. Jany, R. Fawzi, M. Steimann, Organometallics 13 (1994) 647.
[11] B. Rieger, G. Jany, R. Fawzi, M. Steimann, Z. Naturforsch. 49b (1994) 451.
[12] B. Rieger, G. Jany, Chem. Ber. 127 (1994) 2417.
[13] G. Jany, R. Fawzi, M. Steimann, B. Rieger, Organometallics 16 (1997) 544.
[14] G. Jany, T. Repo, M. Gustafsson, M. Leskelä, M. Polamo, M. Klinga, U. Dietrich, B. Rieger, Chem. Ber. 130 (1997) 747.
[15] G. Jany, M. Gustafsson, T. Repo, M. Klinga, M. Leskelä, Acta Cryst. C53 (1997) 644.
[16] T. Repo, M. Klinga, M. Leskelä, M. Polamo, B. Rieger, Acta Cryst. C52 (1996) 2910.
[17] C. Kowala, J.A. Wunderlich, Acta Cryst. B32 (1976) 820.
[18] T. Repo, M. Klinga, I. Mutikainen, Y. Su, M. Leskelä, M. Polamo, Acta Chem. Scand. 50 (1996) 1116.
[19] L. Resconi, R.L. Jones, A. Rheingold, G.P.A. Yap, Organometallics 15 (1996) 998.
[20] U. Plöcker, H. Knapp, J. Prausnitz, Ind. Eng. Chem. Process Des. Rev. 17 (1978) 324.
[21] T.N. Tyvina, G.D. Efremova, R.O. Pryanikova, Russ. J. Phys. Chem. 47 (10) (1973) 1513.
[22] W. Krauss, W. Gestrich, Chem. Tech. 6 (1977) 513.
[23] L. Resconi, F. Piemontesi, G. Franciscono, L. Abis, T. Fiorani, J. Am. Chem. Soc. 114 (1992) 1025.
[24] B. Rieger, Polym. Bull. 32 (1994) 41.
[25] P. Burger, K. Hortmann, H.H. Brintzinger, Macromol. Chem., Macromol. Symp. 66 (1993) 127.
[26] W. Ried, W. Merkel, H.J. Herrmann, Liebigs Ann. Chem. 91 (1971) 750.
[27] K. Komatsu, R. Fujiura, K. Okamoto, Chem. Lett. (1988) 451.
[28] G.M. Sheldrick, SHELXTL/PC, Version 4.2. Siemens Analytical X-ray Instruments Inc., Madison, WI, USA, (1990).
[29] G.M. Sheldrick, SHELXL-93, Program for the Refinement of Crystal Structures, Univ. of Göttingen, Germany, (1993).